Effect of Electrostatic Interaction on the Characteristics of Compound-induced Soy Protein Isolates Gels

[1, a]Ping Du, [3, a]Xingjian Huang, [3]Siyi Pan and [2, 4*]Fang Yang
[1]Research Center for Analysis and Measurement, Kunming University of Science and Technology, Kunming 650093, China
[2]Key Laboratory for Green Chemical Process of Ministry of Education, Wuhan Institute of Technology, Wuhan 430073, China
[3]College of Animal Science and Technology, Huazhong Agricultural University, Wuhan 430070, China
[4]Department of Animal and Food Sciences, University of Kentucky, Lexington, KY 40546, USA

Abstract: The effect of electrostatic interaction on the state of water in compound-induced soy protein isolate gels was investigated in this study. The state of water in SPI gels was analyzed using Differential Scanning Calorimetry (DSC) and Thermogravimetry (TG). Meanwhile Texture Profile Analysis (TPA) was used to analyze the texture properties of SPI gels with different electrostatic interactions. Furthermore, the interactive mechanism at microscopic and molecular level was investigated by means of Scanning Electron Microscopy (SEM), Raman spectrum and Circular Dichroism (CD) spectrum. The results showed that the Equilibrium Water Content (EWC) reduced, gel hardness reduced and gel pore size became smaller with improved electrostatic interaction in compound-induced SPI gels. EWC exhibited the positive correlation with hardness (r = 0.978, p<0.05) and springiness (r = 0.953, p<0.05) of the compound-induced SPI gels. Electrostatic interaction of compound-induced SPI gels seems to point toward its important role in defining their state of water, texture properties and gel structure.

Keywords: Microscopic structure, SPI gel, state of water, static electricity, texture properties

INTRODUCTION

In many foods, proteins play a major role in product quality and determine many of the functional properties of these systems (Gerrard, 2002). Not only does soybean provide an excellent source of dietary protein and fiber, it also offers numerous health benefits. Clinical studies have shown that consumption of soy proteins may reduce the risk of cardiovascular diseases, certain types of cancers and osteoporosis (Messina, 1999). Tofu, one of the Chinese traditional foods, is also known as soybean curd. It is prepared by curdling soymilk with proper coagulants and is arguably the most popular gel-type soy food (Tseng and Xiong, 2009). Zhongxiang Tofu is known for its unique taste, good tenacity and rich nutrition with a long history of manufacturing and it is made through soaking, milling, filtration, boiling and adding calcium sulfate dihydrate at 80°C. Then the whole block is sliced into small chunks (about 8 cm^2, 3 cm thick) and packed with organza. Finally the water is extruded out of the blocks.

Many previous studies have focused on the influence of additive components on the soybean protein gels. Tseng and Xiong (2009) investigated the rheological properties of inulin-containing silken tofu coagulated with Glucono-δ-Lactone (GDL) upon heating. The results indicated that inulin enhanced the viscoelastic properties of GDL-coagulated silken tofu and the textural effect provided by the inulin being an added benefit to its current application which was mainly as a prebiotic ingredient in food. Emiko (2003) studied the effects of different kinds of sesame materials on the physical properties of gomatofu by rheological measurements, sensory evaluation and by SEM. It was shown that the gomatofu prepared by using different sesame materials resulted in different textures. Chang et al. (2003) found that the gel properties of tofu depended on the curdling agent and method used for its preparation. The addition of chitosan increased its gel strength, storage stability and, at the same time slightly changed the water holding capacity of tofu gel structure. The microstructure of gels formed from thermally denatured whey proteins varied substantially depending on the level of salts present prior to heating (Foegeding et al., 1995; Langton and Hermansson, 1992).

Electrostatic interaction, which can be changed by adjusting the ionic strength of the protein gel, has a

Corresponding Author: Fang Yang, Key Laboratory for Green Chemical Process of Ministry of Education, Wuhan Institute of Technology, Liufang avenue 19, Jiangxia District, Wuhan, Hubei 430073, P.R. China, Tel.: +86-027-87194932; Fax: +86-027-87194853

significant effect on protein gel. As one of the important components in the soybean protein gels, salt can change electrostatic interaction of protein gel. The effects of salts on protein structure involve two mechanisms. The first is the effect of the electrostatic shielding only depending on the ionic strength of the medium and not on the nature of the ion. The second is that salts exert ion-specific effect on hydrophobic interactions and affect the stability of proteins at higher concentration (Cheng and Srinivasan, 1991). Errington and Foegeding (1998) performed a detailed study of the influence of salts on the microstructure properties of the thermally induced whey gels and concluded that the microstructure of protein gel was a fine-stranded network. The electrostatic repulsion between Protein Molecule Chains (PMCs) would prevent them from aggregating. In addition, other locations such as hydrophobic patches on the PMCs would promote the PMCs to aggregate. The fine-stranded network was formed when the prevention and promotion forces reached a balance (Barbut, 1995; Doi, 1993; Record *et al*., 1998; Tang *et al*., 1993; Verheul and Roefs, 1998). Different sources and different formation mechanisms of protein gels were affected by electrostatic interactions differently. During the Chinese tofu processing, factors that lead to protein denaturation are complex and include heating and calcium sulfate. Therefore, it is called compound-induced gel. Studies on the effect of electrostatic interaction on compound-induced gel properties are less.

Circular dichroic analysis of protein fluid expressed from globular protein gels at high centrifugal force has been used to elucidate the structural state of globular proteins in gels (Kuhn and Foegeding, 1991). Since neutral salts, such as NaCl, have salting-out effect when their concentrations are above 0.15 M, the solubility will be decreased (Guerrero *et al*., 2004). In this study, the sodium chloride concentrations added to the SPI were 0, 0.025, 0.050 and 0.075 mol/L, respectively to explore the SPI gels with different electrostatic interactions. The purpose is to get the higher quality and stability of Chinese tofu through adjusting the electrostatic interaction. DSC and TPA were used to analyze the state of water and texture properties of the SPI gels. Furthermore, the influence of electrostatic interaction on the state of water and texture properties was discussed. Raman spectrum and CD were used to investigate the structure of gels with different electrostatic interactions. In addition, SEM was used to analyze the microstructure of the SPI gels.

MATERIALS AND METHODS

Materials: SPI was native and provided by Shandong Yuwang Ltd., China. The mean moisture, protein, fat and ash content were 6.0, 91.0, 0.5 and 3.5%, respectively. Sodium hydroxide, calcium sulfate dehydrate ($CaSO_4 \cdot 2H_2O$), sodium chloride and hydrochloric acid were obtained from Sigma. Distilled water was used and all the reagents used were analytical grade.

Preparation of SPI gels interfused with electrostatic interactions: The apparatus and procedures for preparation of SPI gels interfused with different contents of Na^+ were similar to those used previously to obtain a series of SPI solution with different electrostatic interactions (Yang *et al*., 2010). First, three independent tests (replications) were performed and in each replication, the prepared SPI dispersion (12% w/v, pH 6.7) was poured into glass beakers (50 mL in each beaker). Second, NaCl with the final concentration of 0, 0.025, 0.050 and 0.075 mol/L, respectively was added to the beakers. Third, the pH of all samples was adjusted to 7.5 by sodium hydroxide (2 mol/L) and hydrochloric acid (1 mol/L). Then the samples were subjected to thermal processing according to the reference's procedures (Clark and Lee, 1986). This mixture was heated up to its boiling point in a pan on a stove with continuous stirring and then kept boiling for 2.5 min. After cooling down to 80°C, the solution of calcium sulfate dihydrate, which was obtained by dissolving 0.24 g calcium sulfate dihydrate in 5 mL water, was added to 25 mL cooled mixture with stirring for 1 min to make a final concentration of 0.8% w/v calcium sulfate dihydrate (Nakamura *et al*., 1986). Finally, the beakers were sealed with plastic caps and the SPI gels were formed by heating the glass beakers at 80°C in a water bath for 50 min.

Measurement of Swelling Rate (SR): The apparatus and procedures for the measurement of swelling rate were similar to those used previously (Yang *et al*., 2010). Freeze-dried gel samples were weighed, which was noted as W_d. The sample was put into plastic cups with a nylon bottom and kept in water until the sample became fully saturated with water. Each cup was removed from the water and the exterior water was sieved. The freeze-dried gel samples were weighed again. The above operations were repeated until the wet weight of gel samples was constant. The constant weight value was noted as W_s. Finally, the SR and the EWC were calculated from the following formula:

$$SR = (W_s - W_d)/W_d \qquad (1)$$

$$EWC = (W_s - W_d)/W_s \qquad (2)$$

Differential scanning calorimetric measurements: The apparatus and procedures for Differential Scanning Calorimetric measurements (DSC) were similar to those used previously (Yang *et al*., 2010). First, five milligrams gel samples were weighed into an aluminum pan (Dupont). Second, the pan was sealed and heated from -60 to 110°C at a rate of 5°C/min with the safeguard of nitrogen with the speed of nitrogen airflow 40 mL/min.

Given that the enthalpy value (ΔH) of water in gels equals to the ΔH of pure water, 334 J/g, the content of frozen water can be calculated from the enthalpy by 0°C in DSC figure (W_{fro}, equals to the sum of free water (W_f) and intermediate water (W_{in})):

$$W_{fro} = W_f + W_{in} = (\Delta H/\Delta H_0) \times 100\% \qquad (3)$$

The content of frozen water subtracted from total EWC gives the content of non-frozen water:

$$W_{nf} = EWC - W_{fro} = EWC - (W_f + W_{in}) = EWC - [\Delta H/\Delta H_0] \times 10 \qquad (4)$$

where,

ΔH (J/g) : The enthalpy change per mass, is obtained by the calculation of the endothermic peak from DSC

ΔH_0 : The enthalpy change per mass of pure water (J/g)

Thermogravimetry measurements: The apparatus and procedures for thermogravimetry measurements were similar to those used previously (Yang *et al.*, 2010). Thermogravimetric analysis was carried out on a PerkinElmer TGA instrument. The temperature range was from 20 to 480°C with a heating rate of 5°C/min and the experiments were carried out in nitrogen atmosphere.

Texture profile analysis: The apparatus and procedures for Texture Profile Analysis (TPA) were similar to those used previously (Yang *et al.*, 2010). An Instron machine (TA.XT. plus, U.K.) was used to investigate the texture of SPI gels, which were obtained by adding different contents of Na^+ to obtain a series of solutions with different electrostatic interactions. The samples were compressed axially between two parallel plates to 30% of the original height (70% deformation) in two consecutive cycles at a crosshead speed of 2.00 mm/sec. The measurement conditions were as follows: Mode and option: TPA, Pre-Test speed: 2.00 mm/sec, Test speed: 2.00 mm/sec, Post-Test speed: 2.00 mm/sec, Test distance: 30% thickness of the gel, Interval of two tests: 3.00 sec, Trigger Type: Auto, Trigger Force: 5.0 g and Probe Type: P/6.

Raman spectrum analysis: The apparatus and procedures for Raman Spectrum Analysis were similar to those used previously (Yang *et al.*, 2010). Raman spectrum was performed using the FT-Raman spectrometer and the sample was freeze-dried. The measurement conditions were as follows: the light source was diode infrared source of 1064 nm, laser power of 150 mW, scanning times of 50, resolution of 4 cm^{-1} and wave number of 3500-50 cm^{-1}, respectively.

CD spectrum analysis: The apparatus and procedures for CD Spectrum Analysis were similar to those used previously (Yang *et al.*, 2010). Three milligrams of the freeze dried gel sample were dissolved in 3 mL distilled water (concentration of protein was 1 mg/mL). Then the freeze-dried gel solution was centrifuged (Beckman Model L-2 ultracentrifuge) at 35000 rpm for 1 h at 5°C. The solution was infused into the quartz cell and scanned by the circular dichroism spectrum instrument (Jasco810).

Scanning electron microscopy: The morphology of the sample was characterized by Scanning Electron Microscopy (SEM) (model S-4700; Hitachi Co., Japan). Specimens were prepared by the method of Inoue and Osatake (1988). First, the SPI gel was cut into blocks (3×3×3 mm) to immers 3 mL of 2.5% glutaraldehyde in 0.1 M phosphate buffer (pH 7.4) for 1 h at 4°C. Second, the pre-fixed sample was rinsed twice in 0.1 M phosphate buffer (pH 7.4), followed by post-fixing in 1% osmium tetroxide solution. Then the sample was dehydrated by 60, 70, 80, 90, 95 and 99.5%, respectively of ethanol and transferred to *t*-butyl alcohol. The sample in *t*-butyl alcohol was placed in a freezer. The frozen sample was then transferred into the bell jar of a vacuum evaporator to sublimate *t*-butyl alcohol and the temperature fell to -50°C. After sublimation, the dried sample was coated with Au-Pd to produce a specimen in an ion beam sputtering system using argon gas. The specimen was examined by a scanning electron microscope.

Statistical analysis: All data were expressed using the mean±standard deviation (n = 3). Degree of variation and significance of difference were analyzed using Analysis of Variance (ANOVA) that was made with the General Linear Model procedure to determine the treatment effects. Significant ($p<0.05$) differences between means were identified by the Least Significant Difference (LSD) procedure.

RESULTS AND DISCUSSION

Effect of electrostatic interactions on the state of water of the compound-induced SPI gels: The ability of SPI gels to hold water is strongly influenced by the microstructure formed under different ionic strength conditions (Barbut, 1995). Na^+ was added into the SPI gels to change the electrostatic interactions and ionic strength conditions. We focused on the influence of electrostatic interactions on the water state of the SPI gels using the SR analysis, DSC analysis and TG analysis.

Effect of electrostatic interactions on the SR and EWC of the compound-induced SPI gels: The SR of the compound-induced SPI gels at 0, 0.025, 0.050 and 0.075 mol/L, respectively sodium ion was determined to be 4.48±0.21, 3.01±0.12, 2.62±0.15 and 2.28±0.11, respectively. From Table 1, we can see that the EWC

Table 1: The state of water in compound-induced SPI gel with different electrostatic interactions

Final concentration of Na$^+$ (mol/L)	Equilibrium water content, EWC (% w/v)	Frozen water, W_{fro} (% w/v)	Non-freezing water, W_{nf} (% w/v)
0	81.10±4.06[a]	72.21±3.61[a]	8.89±0.45[a]
0.025	77.90±3.89[b]	69.87±3.49[a]	8.03±0.32[a]
0.050	73.87±2.95[c]	69.49±3.47[a]	4.38±1.18[c]
0.075	70.02±2.81[d]	63.84±3.19[a]	6.18±0.31[b]

[a-d]: Means (n = 3) ±standard deviations within a column with different superscripts differ significantly (p<0.05)
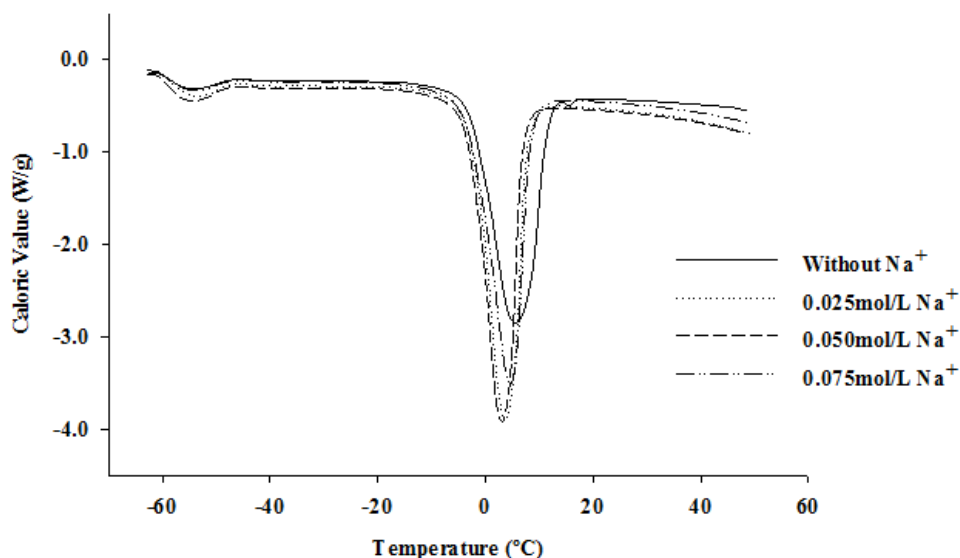

Fig. 1: DSC spectrum of compound-induced SPI gel with different electrostatic interactions by adding different contents of Na$^+$

were reduced significantly with the addition of Na$^+$ which indicates that the additional Na$^+$ and higher ionic strength could make the gel network structure more compact and fine-stranded (Withida and David, 2002). Frozen water has no significant change with the addition of Na$^+$. When sodium ions content is 0.050 and 0.075 mol/L, the non-freezing water of the SPI gel is significantly lower than that without the addition of sodium ion, which shows that the addition of sodium ion can reduce the non-freezing water content.

The EWC corresponds to the content of water in the cave diameter. The additional Na$^+$ reduced the electrostatic repulsion between the protein molecules, resulting in the more compact PMCs. The formed structure which had smaller size pores was more fine-stranded. Hence the capability of holding water decreased during the gel forming process, leading to the reduction of the SR and EWC.

DSC analysis on effect of electrostatic interactions on the compound-induced SPI gels: The Differential Scanning Calorimeter was used to analyze the state of water of the compound-induced SPI gels with different contents of Na$^+$. The chart of DSC measurement by origin soft is shown in Fig. 1. The content of Na$^+$ of the compound-induced SPI gels was positively correlated with the equilibrium water content (r = -0.999, p≤0.001). This may possibly be due to the electrostatic

shielding effect which reduced the water holding capacity of the compound-induced SPI gels. The content of frozen water (p = 0.073) and non-frozen (p = 0.243) water were not positively correlated with the addition of Na$^+$ (Table 1).

TG analysis on effect of electrostatic interactions on the compound-induced SPI gels: TG analysis was used as an auxiliary method to analyze the state of water of the SPI gels. TG analysis showed that the SPI gel has 2 separate weight-loss regions. The free water was lost first, then the intermediate water was lost and finally the non-freezing water was lost when the temperature rose from 20°C.

Various states of water were analyzed using the DSC patterns and the TG patterns. The consistency of the EWC and the weight-loss rate based on the DSC patterns and the first weight-loss region of TG patterns, respectively, showed that the second weight-loss region of TG patterns corresponds to the thermal decomposition and denaturation of dry SPI gel.

The textural properties of the SPI Gels with different electrostatic interactions: The textural properties of SPI gels play an important role in terms of quality and consumer acceptability. Texture profile analysis was carried out to reveal the link between the

Table 2: Effect of electrostatic interactions on the texture properties of compound-induced SPI gels

Final concentration (mol/L)	Hardness (N)	Springiness	Adhesiveness (g·sec)	Cohesiveness
0	3.60±0.16[a]	1.32±0.07[a]	3.24±0.17[b]	0.49±0.03[a]
0.025	3.40±0.17[a]	1.12±0.05[b]	5.02±0.28[a]	0.45±0.04[ab]
0.050	2.10±0.08[b]	1.08±0.07[bc]	4.95±0.33[a]	0.45±0.03[ab]
0.075	1.40±0.07[c]	0.96±0.04[c]	3.50±0.17[b]	0.40±0.02[b]

[a-c]: Means (n = 3) ±standard deviations within a column with different superscripts differ significantly (p<0.05)

structural characteristics and the textural properties. Peak values from the first and the second compressions were designated as peak A force and peak B force, respectively. Peak A force was designated as "hardness" of the sample. Springiness (distance the sample recovered after the first compression, dimensionless) was the degree to which the sample returns to its original size after partial compression. Adhesiveness was defined as the negative force area for the first bite and represents the work required to overcome the attractive forces between the surface of food and the surface of other materials with which the food comes into contact, i.e., the total force necessary to pull the compression plunger away from the sample. Sample "cohesiveness" (total area of peak B divided by total area of peak A), as defined by Bourne (1978), was computed by dividing the squared peak B value by the squared peak A value (because peaks A and B were similar in shape) (Xiong *et al.*, 1999).

As shown in Table 2, the texture of compound-induced SPI gel samples varied with the addition of Na^+. It shows that SPI gel hardness was significantly reduced as Na^+ content increased (r = -0.968, p<0.05); so were the springiness (r = -0.966, p<0.05) and cohesiveness (r = -0.946, p≤0.05); while adhesiveness (r = -0.098, p = 0.0902) was not correlated with the Na^+ content in the SPI gel. We concur that the electrostatic force was influenced with the addition of Na^+. Doi (1993) explained that how proteins were assembled into fine-stranded structures because they only had a limited number of hydrophobic patches on their surface where they can link to neighboring protein molecules. At the same time, interactions at other locations on the protein surface were prevented between the protein molecules (Withida and David, 2002). The electrostatic force played a role in the aggregation of the PMCs and the formation of the compound-induced SPI gel network. Particular networks were formed when the electrostatic repulsion between the protein molecules was relatively weak, i.e., when the proteins had a low net charge (near their isoelectric point) and/or when the solution ionic strength was high enough to screen electrostatic interactions. Na^+ reduced the electrostatic repulsion and the PMCs closely aggregated and the compound-induced SPI gels network structure became more compact. At the same time, the more compact network restrained the frozen water from further migrating into the gel network. Therefore, the textural properties varied because of the reduction of the frozen water in

the compound-induced SPI gels. This is consistent with the results from research on the milk system where with increasing ionic strength, protein affinity for water is increased, thus the hardness of the gel reduced (Daviau *et al.*, 2000).
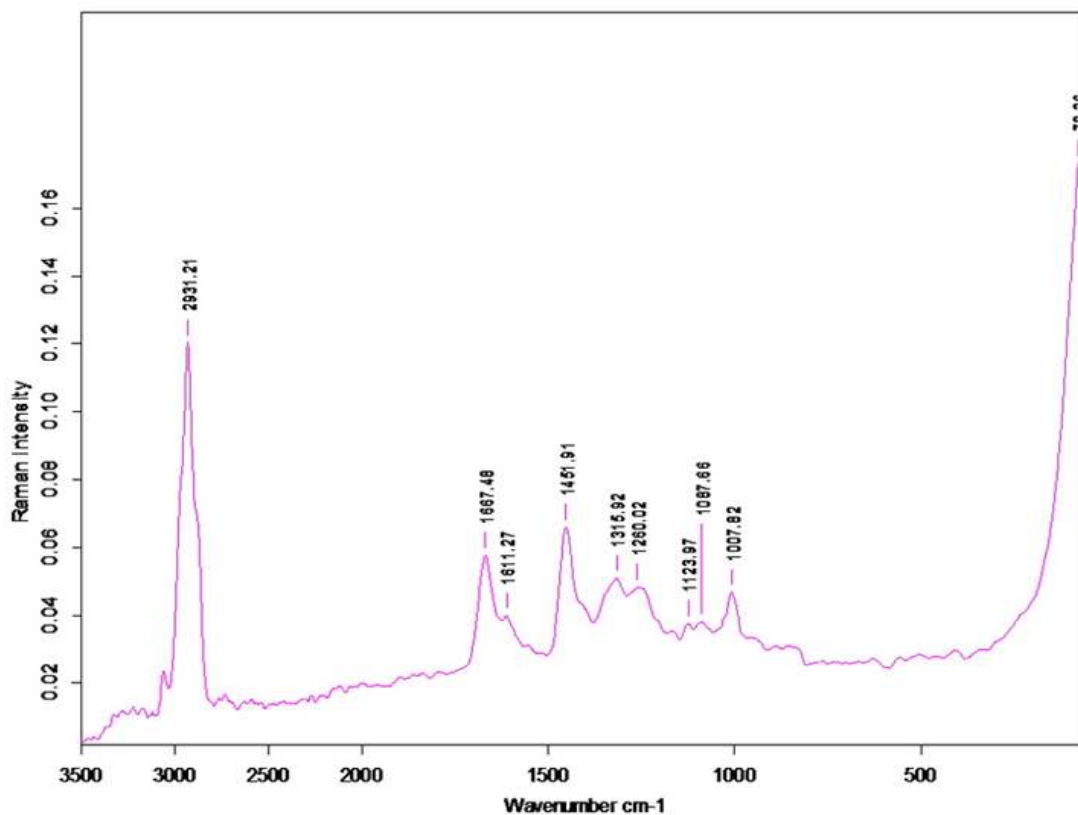
The soy protein secondary structure in SPI gels with different electrostatic interactions
Raman spectrum analysis on the SPI gels with different electrostatic interactions: The Raman spectrum analysis shows the effect of Na^+ on compound-induced SPI gels. Characteristics of the gel sample conformation are clearly defined through the synthetical analysis of amide Ⅲ and amide I Raman region. According to Qiu and Chen (2001): α-helix: $1264\text{-}1310 \text{ cm}^{-1}$, β-sheet: $1230\text{-}1245 \text{ cm}^{-1}$, β-turn: $1254\text{-}1300 \text{ cm}^{-1}$, random coil: $1242\text{-}1250 \text{ cm}^{-1}$.

Figure 2a represents the Raman spectrum of the freeze-dried SPI gel sample without Na^+. The Raman peaks in the amide Ⅲ region appeared at 1260 and 1315 cm^{-1}, we conclude that 1260 cm^{-1} peak (I = 0.042) corresponds to β-sheet; 1315 cm^{-1} (I = 0.048) peak corresponds to α-helix. Figure 2a shows that the peak area at 1667 cm^{-1} is larger than that at 1260 cm^{-1}, indicating that 1667 cm^{-1} peak (I = 0.030) corresponds mainly to β-sheet and β-turn. In summary, there are α-helix, β-sheet, a small quantity of β-turn and random coils in the samples. Perhaps α-helix and β-sheet are two of the important factors contributing to gel configuration stability.

Figure 2b represents the Raman spectrum of the freeze-dried SPI gel sample with 0.050 mol/L Na^+. The Raman peak of the sample in amide I region reached 1666 cm^{-1}, which indicated that there were β-turn, β-sheet and random coils in the sample. Similar results were obtained from the characteristic vibratory frequency of the amide III region.

Because the Raman peaks in the amide III region appeared at 1238 and 1335 cm^{-1}, we conclude that 1238 cm^{-1} peak (I = 0.030) corresponds to β-sheet; 1335 cm^{-1} peak corresponds to α-helix. Figure 2 shows that the peak area at 1666 cm^{-1} is larger than that at 1238 cm^{-1}, indicating that 1666 cm^{-1} peak (I = 0.030) corresponds mainly to β-sheet. In summary, there are α-helix, β-sheet and a small quantity of β-turn and random coils in the samples and the content of α-helix increased appreciably with the additional Na^+. Perhaps α-helix and β-sheet are two of the important factors

(a)
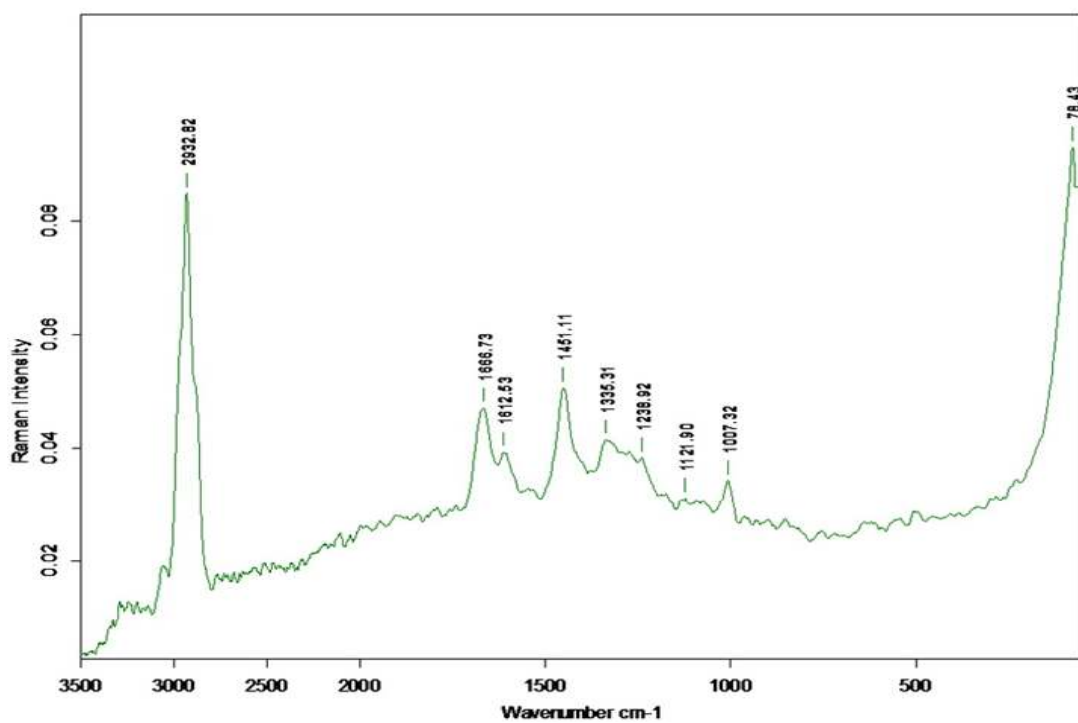
(b)

Fig. 2: Raman spectrum of compound-induced SPI gels. (a) Raman spectrum of SPI gels without Na^+, (b) Raman spectrum of SPI gels with 0.050 mol/L Na^+
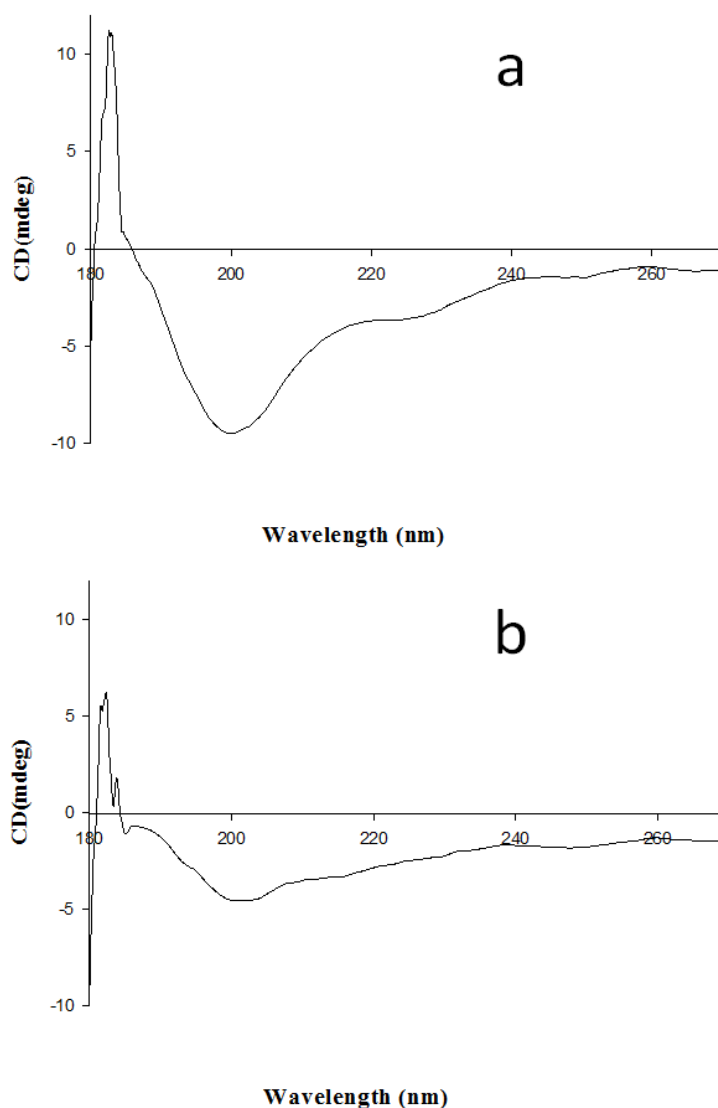
Fig. 3: CD spectrums of compound-induced SPI gel. (a) CD spectrum of compound-induced SPI gel without Na$^+$, (b) CD spectrum of compound-induced SPI gel with 0.050 mol/L Na$^+$

contributing to gel configuration stability. CD spectrums can provide additional necessary information.

CD spectrum analysis on the compound-induced SPI gels with different electrostatic interactions: CD spectrums of the compound-induced SPI gel without Na$^+$ and with 0.050 mol/L Na$^+$ are shown in Fig. 3. The measurement conditions were as follows: Cuvette of 1 mm used for the far ultraviolet CD, sensitivity of 10 mdeg, scanning velocity of 500 nm/min, response time of 1 sec, silt width of 1.0 nm and scanning extension of 180-350 nm. The secondary structure was calculated by the Jasco SSE-338 software using a value of 115 for the mean residue molecular weight. The JascoSSE-338 software analysis showed that the proportion of α-helix, β-sheet, β-turn and random coil in the SPI gel without Na$^+$ were 4.9, 33.0, 14.6 and 47.5%, respectively. From

Fig. 3b we concluded that there were two positive peaks at 183 and 184 nm in the CD spectrum pattern with a negative peak appearing at 203 nm. This peak was similar with the β-sheet peak which indicated there were many β-sheet structures in the sample. The shift of the peak from 215 to 203 nm can be explained by the presence of β-turn, α-helix and random coil. The JascoSSE-338 software analysis showed that the proportion of α-helix, β-sheet, β-turn and random coil in the SPI gel with 0.050 mol/L Na$^+$ are 11.2, 23.5, 19.4 and 45.9%, respectively. The proportions of β-sheet showed a downward trend with the addition of Na$^+$ which was in agreement with the results of Raman spectrum analysis. The downward trend of β-sheet indicated that the addition of Na$^+$ would result in the more compact gel configuration, creating a change of the cave diameter. This affects the state of water of gel system indirectly.

Table 3: Correlation coefficients of the texture properties with the state of water of the compound-induced SPI gels (n = 3)

Texture properties	Equilibrium water content, EWC (% w/v)	Frozen water, W_{fro} (% w/v)	Non-freezing water, W_{nf} (% w/v)
Springiness	0.978*	0.879	0.791
Adhesiveness	0.953*	0.908	0.681
Cohesiveness	-0.057	0.160	-0.419
Hardness	0.939	0.980*	0.519

*: $p < 0.05$

(a)   (b)

(c)   (d)
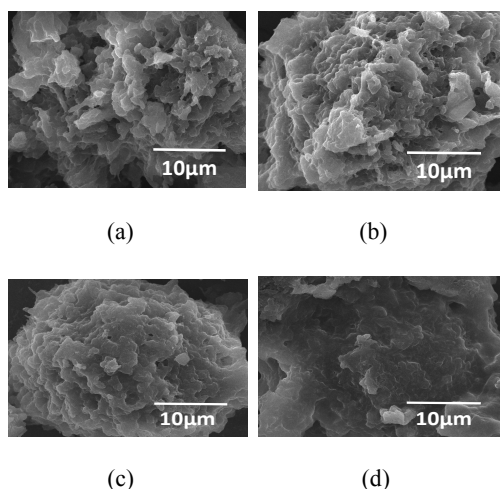
Fig. 4: Scanning electron microscopic image of SPI gel samples (×2000). SPI gel samples were prepared by adding different contents of Na^+: the Figure a, b, c and d represented the scanning electron photos of Na^+ at the contents of 0, 0.025, 0.050 and 0.075 mol/L, respectively

Scanning electron microscopic structure: To further confirm the influences of Na^+ on the microstructure of the calcium sulfate dihydrate induced SPI gels, we investigated the microstructure of SPI gels treated at different contents of Na^+, as shown in Fig. 4.

As expected, the SEM images of SPI gels prepared with different contents of Na^+ show different microstructures in size and density of the particles among the gel samples. The cave diameters were becoming smaller when the Na^+ concentration was increased.

We came to the conclusion that the additional Na^+ led to the reduction of the electrostatic repulsion, thus promoting the association of the PMCs. The more fine-stranded structures with small pore sizes were associated which made the network structure of SPI gels more compact (Barbut, 1995). The results and analysis were consistent with the conclusions of the study about the influence of salt on the microstructure of protein gels (Kuhn and Foegeding, 1991).

Correlation between the texture properties and the state of water of the compound-induced SPI gels: There was no significant correlation between adhesiveness and the equilibrium water content of the compound-induced SPI gels. Similarly, no distinct correlation was found between cohesiveness and the equilibrium water content of the compound-induced SPI gels (Table 3). However, hardness (r = 0.978, $p < 0.05$) and springiness (r = 0.953, $p < 0.05$) were both positively correlated with the equilibrium water content of the compound-induced SPI gels (Table 3). Cohesiveness (r = 0.980, $p < 0.05$) was positively correlated with the frozen water content of the compound-induced SPI gels and the frozen water content had no evident effect on hardness, springiness and adhesiveness of the compound-induced SPI gels. Furthermore, there was no direct relation between non-freezing water content and the texture properties.

CONCLUSION

This study showed that different electrostatic interactions with different Na^+ content could lead to differences in protein structure and gel properties. The equilibrium water content had evident effect on hardness and springiness of the compound-induced SPI gels. Cohesiveness was positively correlated with the frozen water content of the compound-induced SPI gels. There was no direct relation between non-freezing water content and the texture properties. With the additional Na^+, the state of water exhibited an effect on the texture properties of SPI gels. The SEM results showed that the additional Na^+ made the network structure more compact and the cave diameter of the SPI gels tended to become smaller with increased Na^+ content. The CD and Raman analysis showed an increase of the contents of α-helix and a decrease of the contents of β-sheet with the additional Na^+. As a result, we can change water state and textural properties of soy protein gel by adding low doses of sodium ions to improve the quality of compound-induced tofu products without changing the basic flavor and there is no security problem.

ACKNOWLEDGMENT

REFERENCES

Barbut, S., 1995. Effect of sodium level on the microstructure and texture of whey protein isolate gels. Food Res. Int., 28: 437-443.

Bourne, M.C., 1978. Texture profile analysis. Food Technol., 32(7): 62-66.

Chang, K.L.B., Y.S. Lin and R.H. Chen, 2003. The effect of chitosan on the gel properties of tofu (soybean curd). J. Food Eng., 57: 315-319.

Cheng, H.W. and D. Srinivasan, 1991. Thermal gelation of globular proteins: Influence of protein conformation on gel strength. J. Agric. Food Chem., 39(3): 432-438.

Clark, A.H. and T.C.D. Lee, 1986. Gelation of Globular Proteins. In: Mitchell, J.R. and D.A. Ledward (Eds.), Functional Properties of Food Macromolecules. Elsevier Applied Science Publishers, New York, pp: 203-272.

Daviau, C., M.H. Famelart, A. Pierre, H. Goudédranche and J.L. Maubois, 2000. Rennet coagulation of skim milk and curd drainage: Effect of pH, casein concentration, ionic strength and heat treatment. Lait, 80(4): 397-415.

Doi, E., 1993. Gels and gelling of globular-proteins. Trends Food Sci. Tech., 4: 1-5.

Emiko, S., 2003. Effects of different kind of sesame materials on the physical properties of gomatofu (sesame tofu). Food Hydrocolloid., 17: 901-906.

Errington, A.D. and E.A. Foegeding, 1998. Factors determining fracture stress and strain of fine-stranded whey protein gels. J. Agr. Food Chem., 46: 2963-2967.

Foegeding, E.A., B.L. Bowland and C.C. Hardin, 1995. Factors that determine the fracture properties and microstructure of globular protein gels. Food Hydrocolloid., 9: 237-249.

Gerrard, J.A., 2002. Protein-protein cross-linking: Methods, consequences, applications. Trends Food Sci. Tech., 13: 389-397.

Guerrero, A., J.A. Carmona, I. Martínez, F. Cordobés and P. Partal, 2004. Effect of pH and added electrolyte on the thermal-induced transitions of egg yolk. Rheol. Acta, 43(5): 539-549.

Inoue, T. and H. Osatake, 1988. Complementary observation on fractured intracellular structures, especially the golgi apparatus, by scanning electron microscopy. J. Electron. Microsc., 37(6): 333-336.

Kuhn, P.R. and E.A. Foegeding, 1991. Mineral salt effects on whey-protein gelation. J. Agr. Food Chem., 39: 1013-1016.

Langton, M. and A.M. Hermansson, 1992. Fine-stranded and particulate gels of β-lactoglobulin and whey protein at varying pH. Food Hydrocolloid., 5: 523-539.

Messina, M.J., 1999. Legumes and soybeans: Overview of their nutritional profiles and health effects. Am. J. Clin. Nutr., 70(3): 439-450.

Nakamura, T., S. Utsumi and T. Mori, 1986. Interactions during heat-induced gelation in a mixed system of soybean 7S and 11S globulins (food and nutrition). Agr. Biol. Chem., 50(10): 2429-2435.

Qiu, H.X. and W.C. Chen, 2001. The micro-laman study on rat pallium and veins sphere. Biophys. Trans., 17(3): 457-461.

Record, M.T., W. Zhang and C. Anderson, 1998. Analysis of effects of salts and uncharged solutes on protein and nucleic acid equilibria and processs: A practical guide to recognizing and interpreting polyelectroyte effects, Hofmeister effects and osmotic effects of salts. Adv. Protein Chem., 51: 282-355.

Tang, Q.N., O.J. McCarthy and P.A. Munro, 1993. Oscillatory rheological study of the gelation mechanism of whey-protein concentrate solutions: Effects of physicochemical variables on gel formation. J. Dairy Res., 60: 543-555.

Tseng, Y.C. and Y.L. Xiong, 2009. Effect of inulin on the rheological properties of silken tofu coagulated with glucono-δ-lactone. J. Food Eng., 90: 511-516.

Verheul, M. and S.P.F.M. Roefs, 1998. Structure of whey protein gels studied by permeability, scanning electron microscopy and rheology. Food Hydrocolloid., 12: 17-24.

Withida, C. and J.M. David, 2002. Influence of NaCl on optical properties, large-strain rheological and water holding capacity of heat-induced whey protein isolate gels. Food Hydrocolloid., 16: 467-476.

Xiong, Y.L., D.C. Noel and W.G. Moody, 1999. Textural and sensory properties of low-fat beef sausages with added water and polysaccharides as affected by pH and salt. J. Food Sci., 64: 550-554.

Yang, F., D. Weng, X.J. Huang, X.L. Yao and S.Y. Pan, 2010. Research on the interaction of lipid and protein in SPI gel. Eur. Food Res. Technol., 230: 467-473.